

RESEARCH ARTICLE

Patient-specific targeted bronchial thermoplasty: predictions of improved outcomes with structure-guided treatment

 **Graham M. Donovan,¹ John G. Elliot,² Stacey R Boser,³ Francis H. Y. Green,⁴ Alan L. James,⁵ and Peter B. Noble⁶**

¹Department of Mathematics, University of Auckland, Auckland, New Zealand; ²West Australian Sleep Disorders Research Institute, Department of Pulmonary Physiology and Sleep Medicine, Sir Charles Gairdner Hospital, Nedlands, Western Australia, Australia; ³Cumming School of Medicine, Calgary, Alberta, Canada; ⁴Cumming School of Medicine, University of Calgary, Calgary, Alberta, Canada; ⁵Department of Pulmonary Physiology and Sleep Medicine, Sir Charles Gairdner Hospital, School of Medicine and Pharmacology, University of Western Australia, Australia; and ⁶School of Human Sciences, University of Western Australia, Crawley, Western Australia, Australia

Submitted 31 October 2018; accepted in final form 16 January 2019

Donovan GM, Elliot JG, Boser SR, Green FH, James AL, Noble PB. Patient-specific targeted bronchial thermoplasty: predictions of improved outcomes with structure-guided treatment. *J Appl Physiol* 126: 599–606, 2019. First published January 24, 2019; doi:10.1152/jappphysiol.00951.2018.—Bronchial thermoplasty is a recent treatment for asthma in which ablative thermal energy is delivered to specific large airways according to clinical guidelines. Therefore, current practice is effectively “blind,” as it is not informed by patient-specific data. The present study seeks to establish whether a patient-specific approach based on structural or functional patient data can improve outcomes and/or reduce the number of procedures required for clinical efficacy. We employed a combination of extensive human lung specimens and novel computational methods to predict bronchial thermoplasty outcomes guided by structural or functional data compared with current clinical practice. Response to bronchial thermoplasty was determined from changes in airway responses to strong bronchoconstrictor simulations and flow heterogeneity after one or three simulated thermoplasty procedures. Structure-guided treatment showed significant improvement over current unguided clinical practice, with a single session of structure-guided treatment producing improvements comparable with three sessions of unguided treatment. In comparison, function-guided treatment did not produce a significant improvement over current practice. Structure-guided targeting of bronchial thermoplasty is a promising avenue for improving therapy and reinforces the need for advanced imaging technologies. The functional imaging-guided approach is predicted to be less effective presently, and we make recommendations on how this approach could be improved.

NEW & NOTEWORTHY Bronchial thermoplasty is a recent treatment for asthma in which thermal energy is delivered via bronchoscope to specific airways in an effort to directly target airway smooth muscle. Current practice involves the treatment of a standard set of airways, unguided by patient-specific data. We consider the potential for guided treatments, either by functional or structural data from the lung, and show that treatment guided by structural data has the potential to improve clinical practice.

INTRODUCTION

Bronchial thermoplasty is a relatively recent treatment for asthma in which thermal energy is delivered to the targeted airways via bronchoscope and radiofrequency catheter (3); proximal airways greater than 3 mm in diameter can be treated. The intention of this therapy is that the appropriate delivery of this thermal energy provides effective long-term ablation of the airway smooth muscle (ASM), which is responsible for the excessive and reversible airway narrowing that is seen in asthma (19). Clinical trials have shown bronchial thermoplasty (BT) to be relatively safe and associated with reduced exacerbation rates, use of rescue medication and emergency visits, and increased quality of life scores related to asthma (7, 9, 28), improvements that are sustained over time (35, 40). Somewhat surprisingly, in contrast to its effectiveness in reducing exacerbations, BT has minimal effects on baseline lung function and airway hyperresponsiveness (19). Our recent modeling work offers a resolution to this apparent paradox in that the effects of BT are apparent only under relatively high levels of ASM activation, which are not reached during assessment in the lung function laboratory due to safety considerations. Therefore, reduced exacerbations after BT without change in baseline lung function or airway hyperresponsiveness can be explained by these observations.

However, BT is not successful in all patients. Current clinical practice involves the treatment of a standard set of airways at specific anatomic locations applied across three separate bronchoscopy procedures at one month intervals (3). This approach is essentially performed “blind” in that the choice of which airways to treat is not driven by structural or functional data to detect optimal treatment sites. Given the intrinsic variability of both structure and function in asthma (41), including the variation in the distribution of increased ASM (14), it is unlikely that this standard set of targeted airways will be optimal for all patients. Recent advances in imaging technology offer the prospect that patient-specific data on airway function and structure could improve outcomes of BT by targeting specific airways (5, 17, 22, 34, 38). A targeted BT procedure may improve clinical efficacy and/or reduce the number of bronchoscopic procedures to achieve the same

Address for reprint requests and other correspondence: G. M. Donovan, Dept. of Mathematics, Univ. of Auckland, Private Bag 92019, Auckland Mail Centre, Auckland 1142, New Zealand (e-mail: g.donovan@auckland.ac.nz).

benefit and is a logical extension of efforts to improve BT treatment by patient phenotyping (23).

In this article we explore the potential for patient-specific airway targeting to improve outcomes of BT. Using the recent predictive model (11), we explore two new methods of bronchial thermoplasty: 1) functional image-guided BT (FIG), in which functional flow patterns [e.g., analogous to Xe or He MRI (6, 33)] are used to select low-ventilation segments for treatment; and 2) structure-guided (SG) BT, in which airway structure data is used in concert with a predictive model to determine the targeted airways. Both proposed treatments are compared with current clinical practice (CCP) after a single session of BT or a complete three-session treatment.

METHODS

Additional details on methodology are provided in the APPENDIX.

Predictive model. We use the model described by Donovan et al. (11), based on others' studies (2, 10, 12, 24, 39), to predict flow patterns dependent on underlying structure both before and after simulated BT. We provide an overview of the model here, and the interested reader is referred to the APPENDIX and Donovan et al. (11) for additional details. The model is calibrated using structural airway data from the Prairie Provinces Fatal Asthma Study (15, 16, 18, 31, 37), specifically using total wall area, ASM area, basement membrane perimeter, and anatomic level from $n = 663$ airways obtained from $n = 25$ subjects, with death attributed to asthma and with a confirmed history. Briefly, a statistical model is constructed using a trivariate correlated log-normal distribution to represent total wall area, ASM area, and basement membrane perimeter at each airway order (20); for full details, the reader is also referred to the supplemental material attached to Donovan et al. (11). Independent realizations of this statistical model generate the simulated airway trees. By this approach, a simulated patient cohort of 22 fatal asthma cases was studied. Respiratory impedance to a high-level ASM stimulus (that which simulates the degree of bronchoconstriction that might occur during an exacerbation; details below) was used as an indication of BT effectiveness since reduction in exacerbations and hospitalizations has been the main successful outcome measure in trials of BT (7, 9, 28, 35).

The model examines a single human lung for reasons of computational complexity, choosing the left lung to avoid complicating effects of the untreated right middle lobe (3). In this study, we compare our patient specific methods (further described below) to current clinical practice (CCP) treatment across three full bronchial thermoplasty sessions. Specifically, the standard treatment targets a total of 13 airways, including the lower lobe bronchus, the upper lobe bronchus, the superior division bronchus, and segmental bronchi LB1–10. A single bronchoscopy session represents treatment of the lower lobe only¹.

We assume that treated airways undergo a 75% reduction in ASM mass that has been demonstrated in biopsy studies after BT (4, 29, 30) and that airway wall area is altered by means of the ASM reduction, but we assume that no other changes occur in the airway wall. Impedance is calculated post hoc using the circuit analog approach (26, 36); specifically, we use as our main output measure resistance at 6 Hz, calculated as the real part of the complex impedance. Response rates are calculated as the fraction

of treatments within the cohort, resulting in reduced resistance in the presence of induced ASM tone; the induced tone is assumed to be ~77% of maximum activation, a simulation of the level of ASM activation that might occur during acute bronchoconstriction. This specific value was selected based on the dose-response curves to be near the maximum mean BT response (11).

Functional image-guided BT (FIG). We select airways for functional image-guided treatment as follows. First, pretreatment flow patterns are calculated using the predictive model described above. Using these functional data, assumed to be analogous to Xe or He MRI, we sequentially select bronchi with the lowest relative flow, as well as their proximal flow pathways. The airway target package is selected for each patient in this way until the predetermined number of treated airways is reached. If the entire proximal pathway cannot be added to the treatment package without exceeding the specified number of treatments, the proximal portion of the pathway is selected for treatment, up to the point where the treatment limit is reached. The selected airway target package is then treated in the same way as described above (i.e., a 75% reduction in ASM mass).

Structure-guided BT (SG). Our structure-guided BT uses data on airway structure, coupled with the predictive model, to select the airways that will produce the greatest improvement in function at the specified level of ASM activation. Importantly, this approach is not equivalent to simply selecting the "most remodeled" airways for treatment.

We begin by predicting the control functional flow patterns based on the structural data. We then take advantage of the predictive model to consider isolated treatment of 75 potential target airways and measure the ΔR response for each, and then to rank the priority of each potential target airway according to their response. The final target package is determined by selecting the appropriate number of treatment airways from this ranking, which may extend distally beyond current clinical practice. A final simulation is then performed to assess the likely effectiveness of the proposed target package as a whole as compared with CCP for an equivalent number of treated airways.

RESULTS

Nomenclature. We refer to the treatment variations using the following abbreviations: current clinical practice BT (CCP); one-session (CCP1) and three-session (CCP3) variants; functional image-guided BT (FIG) (1-session and 3-session variants are FIG1 and FIG3, respectively); structure-guided BT (SG); one-session (SG1) and three-session (SG3) variants. Note that CCP3, FIG3, and SG3 all treat the same number of airways. That is, FIG1 and SG1 all involve the same fixed number of airways, and CCP3, FIG3, and SG3 involve three times as many. CCP1 represents treatment of the lower lobe only.

Demonstration of pre- and posttreatment flow patterns are shown in Fig. 1 for a single (simulated) patient for illustrative purposes. Here, we have selected the control (pretreatment) in Fig. 1, *left*; CCP1 in Fig. 1, *middle*; and SG1 in Fig. 1, *right*. Results for other treatments are provided in the APPENDIX (Fig. A1).

The response to treatment in terms of lung resistance (with ASM tone) is shown for each patient in Fig. 2 across the simulated cohort. Figure 2, *top*, shows for each simulated patient the control response (before BT), along with the post-treatment response for each of the six treatment variations. Statistics for the response of the cohort as a whole are provided in the Fig. 2, *bottom*. All treatments are statistically significant versus control; treatment response rates range from 73% for

¹ It is worth noting that, in clinical practice, the three treatment sessions are not divided equally between the two lungs, and this asymmetry is important because we are modeling treatment of the left lung only. In order to maintain appropriate balance between the one-session and three-session treatments, we assume in all targeted treatment cases that the three-session treatment involves three times as many treated airways as the one-session version.

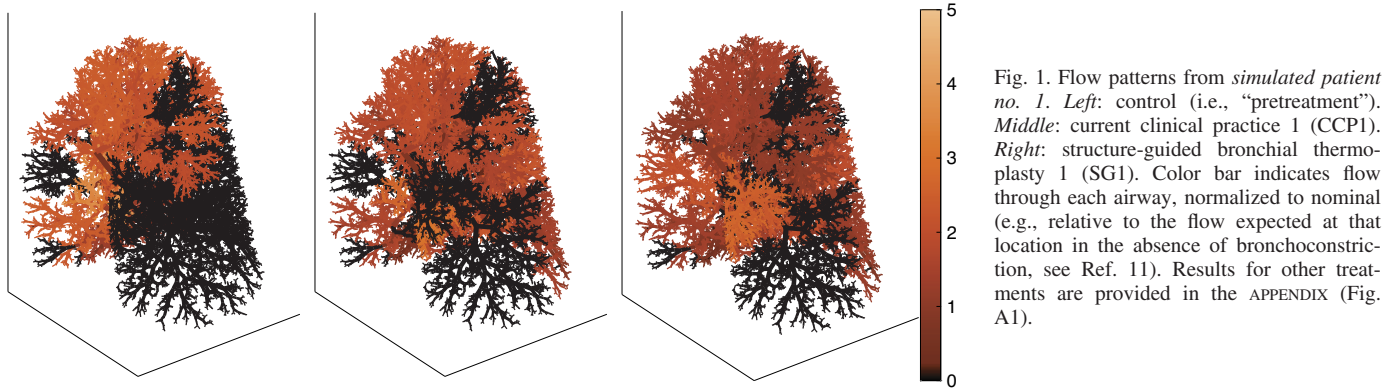


Fig. 1. Flow patterns from *simulated patient no. 1*. *Left*: control (i.e., “pretreatment”). *Middle*: current clinical practice 1 (CCP1). *Right*: structure-guided bronchial thermoplasty 1 (SG1). Color bar indicates flow through each airway, normalized to nominal (e.g., relative to the flow expected at that location in the absence of bronchoconstriction, see Ref. 11). Results for other treatments are provided in the APPENDIX (Fig. A1).

FIG1 up to 86% for SG1 and SG3. SG3 also shows the greatest mean response of all treatments, whereas SG1 shows the largest response within the one-session treatment group. Indeed, SG1 (1 session) shows as much improvement as CCP3 (3 full sessions). Two-way ANOVA indicates significant differences between FIG and SG as well as between one- and three-session treatments.

Responses in terms of the spatial heterogeneity of flow, quantified by the spatial heterogeneity index (SHI; which attempts to capture both heterogeneity and its spatial structure using a combination of the coefficient of variation and

the autocorrelation; see Ref. 11), are shown in Fig. 3. Again, SG3 shows the greatest mean response of all treatments, whereas SG1 shows the largest response within the one-session treatment group.

We also examined the differential response of each patient to each treatment in an effort to assess which treatments might be more advantageous to different patient groups. A summary figure of the differential response is provided in the APPENDIX (Fig. A2). One observation from this analysis is that the response to FIG1, compared with CCP1, varies systematically in patients according to their pretreatment function. Indeed, the

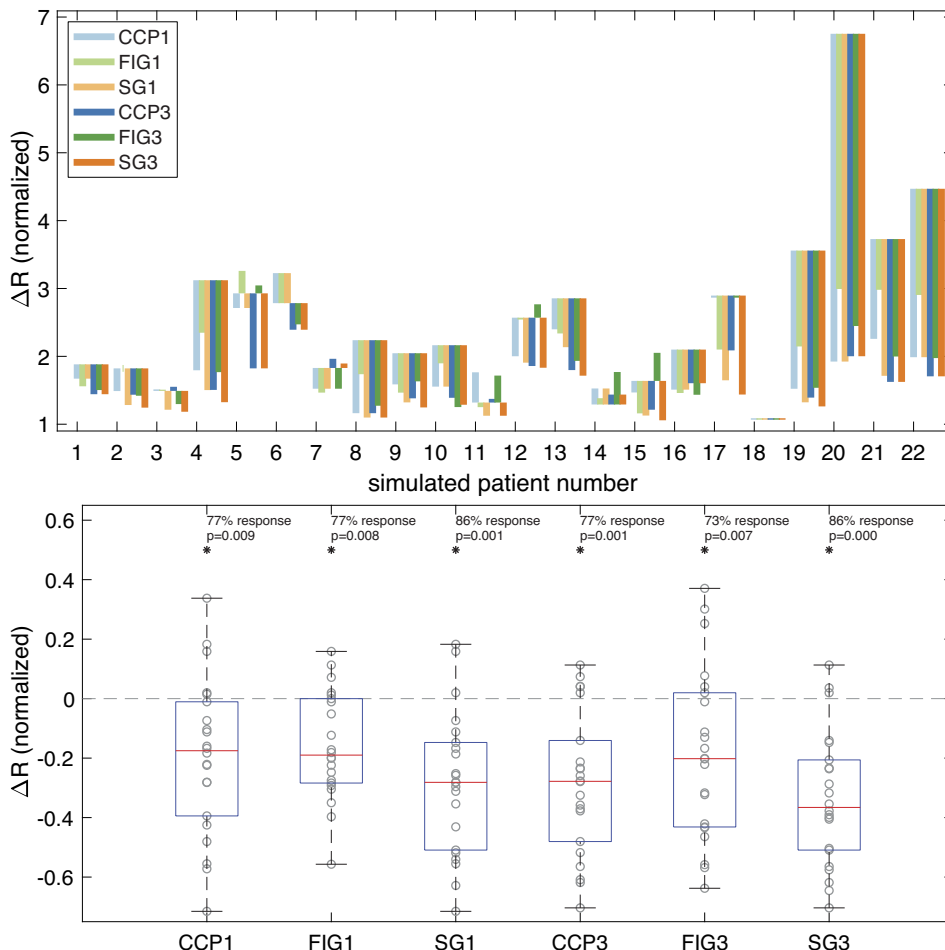


Fig. 2. *Top*: responses to each protocol in each simulated patient in terms of respiratory resistance pre- and posttreatment. Each bar shown indicates the response due to that treatment, with a downward reflection (e.g. all treatments for *patient 1*) indicating improvement in function (majority of cases), whereas an upward reflection (e.g., *patient 5* in FIG1 and FIG3) indicates worsening of function. *Bottom*: statistics of overall response to each treatment across all patients. ΔR indicated the difference in bronchoconstrictor response, with negative values indicating an improvement posttreatment. *P* values shown indicate difference from control by balanced ANOVA; see text for details of 2-way analysis. CCP1 and -3, current clinical practice 1 and 3, respectively; FIG1 and -3, functional image-guided bronchial thermoplasty 1 and 3, respectively; SG1 and -3, structure-guided bronchial thermoplasty 1 and 3, respectively.

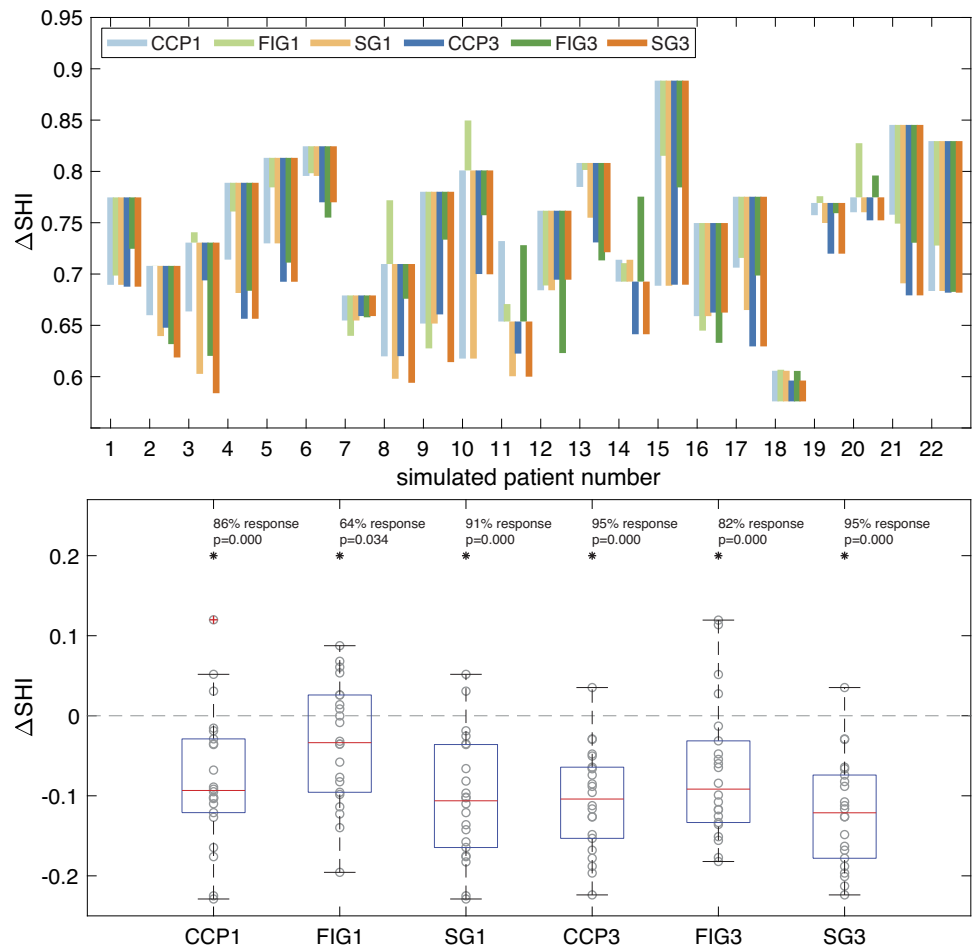


Fig. 3. Response in terms of spatial heterogeneity index (Δ SHI). Details otherwise are as in Fig. 2. CCP1 and -3, current clinical practice 1 and 3, respectively; FIG1 and -3, functional image-guided bronchial thermoplasty 1 and 3, respectively; SG1 and -3, structure-guided bronchial thermoplasty 1 and 3, respectively.

difference in the response to CCP1 and FIG1 is inversely correlated with pretreatment R (control) (Fig. A3).

Finally, a “naïve” form of structure-guided treatment was examined in which the airways with the greatest remodeling, either in terms of total wall area or ASM area (normalized to basement membrane perimeter), were treated; that is, the model was not used to inform the airway targeting. This variant was much less effective than the informed structure-guided treatment, with a <50% response rate (as compared with >85% response rates for the model-informed structure guided treatments).

DISCUSSION

The present study determined whether BT practice could be improved through use of patient-specific functional or structural data in the selection of airways that undergo thermal ablation. We assessed the potential for such patient-specific, targeted treatments, based on either functional or structural data, after one or three treatment sessions. Findings suggest that structure-guided BT holds promise as an improved personalised therapy. One session of structure-guided treatment (SG1) was shown to be as effective as three sessions of current nontargeted treatment (CCP3). Although three sessions of structure-guided treatment (SG3) were more effective than one (SG1), the benefit is perhaps not enough to justify the additional treatments. In comparison, functional image-guided

treatment provided no additional benefit compared with current practice, the reasons for which will be discussed.

The major outcome of the study was that structure-guided BT reduced lung resistance in the presence of ASM tone, as well as ventilation heterogeneity, which was previously suggested to be a primary mechanism behind the efficacy of BT (11). Although it may be intuitive that BT response improves if the physician is aware of and able to treat specific sites of remodeling, it is important to emphasize that neither structure-guided BT nor function-guided BT is equivalent to selecting the “most remodeled” airways for treatment. This is demonstrated by the marked difference in performance between the model-informed structure-guided treatment and the “naïve” form that treats only the most remodeled airways (far less efficacious). In vivo, airways do not operate in isolation. Airways are interdependent because of the distributed nature of the flow patterns across the entire airway tree, as well as the coupling between airways and parenchymal attachments, and dependence of parenchymal tethering forces on local inflation. Conventionally referred to as “airway interdependence,” these effects mean that treatment of one airway indirectly affects the calibre of adjacent airways (13, 27, 42). Therefore, it may not be optimal to treat a severely remodeled airway if upstream and downstream conditions are such that flow through the pathway cannot be significantly improved by the treatment of that airway alone. Using both structural data and the model in

concert allows airway interdependence to be taken into account to design improved BT protocols.

All simulations performed in this study used structural data obtained from fatal asthma cases and considered the resulting function and flow at $\sim 77\%$ of maximal ASM activation. This patient group and level of ASM activation was selected based on our previous findings (11) that differences in function and heterogeneity are not expected to be apparent without ASM tone but only increase with severity of asthma and degree of ASM activation. Because the mechanism of action of BT appears to be consistent between fatal and nonfatal asthma, we expect that results would be similar across patients with different severity. However, perceived clinical severity may be less important than the structural distribution of airway remodeling, which may explain the difficulty in identifying key predictors for BT efficacy (23).

In the present study and a previous study (11), we have used resistance (at 6 Hz) as our measure of function. This requires further elaboration given that BT clinical trials have typically shown consistent improvement in indirect measures such as quality-of-life scores, but not in direct measures of function, i.e., FEV1 (7, 9, 35). As previously, we argue that the changes in function observed in the present mathematical simulation, which are most prominent in more severe asthma and at higher levels of ASM tone, will be difficult to detect in clinical settings because of reduced tolerance to the test; however, such changes would still be expected to manifest through indirect measures such as quality of life scores, exacerbations, and emergency medication use (11). We have used resistance as our measure of function, as opposed to FEV1, not because resistance is necessarily more sensitive to these changes but because resistance models are much better established. The key observation is that baseline measurements of function are much less sensitive than measurements of function during moderate to severe bronchoconstriction. It is also worth emphasizing that we consider only long-term effects, assuming successful ASM ablation (8), after the acute response to treatment has subsided. Indeed one potential benefit to the structure-targeted approach is reducing the number of treatments and hence, the potential severity of the acute response (see below).

An assumption of the study is that perfect information on airway structure is obtainable throughout the airway tree, which is currently impractical. Structural information can be obtained using CT (6), bronchoscopy (32), or OCT (1, 22, 25), but this is likely to be limited to a relatively small number of relatively large airways. Exactly how much data might be plausibly collected, and how much uncertainty this introduces into the structure-guided predictions, remains an open question. In the first instance, it would be pragmatic to base the treatment on data obtained by noninvasive imaging, such as CT, with the understanding that its use as a marker for airway remodeling is under debate (21). With respect to imaging modalities that require a bronchoscopic procedure for the assessment of wall thickness (e.g., OCT), the cost (health and economic) should be weighed against the improved targeting benefits.

The proposed structure-guided treatment approach offers significant savings in both economic and health costs by increasing the effectiveness of the treatment to the point that it is possible to reduce the required number of BT treatment sessions from three to one without compromising the effec-

tiveness of the treatment. The economic benefits therein are self-evident. The health benefits arise in the reduction of the acute and inflammatory response that immediately follows BT treatment and associated complication risks such as hemoptysis or atelectasis (7). Not exposing the patient to the same risk multiple times is an important advantage of the structure-guided approach. Even if bronchoscopic OCT proves necessary to obtain sufficient structural data to guide the treatments, the total number of bronchoscopic procedures required would reduce from three to two, and only one of those would involve thermoplasty.

Greater benefit still is possible using structure-guided BT since the approach taken here is almost certainly not optimal. Although in principle it would be theoretically possible to find a true optimal treatment for each patient, this is not practical given present computational constraints. Our approach demonstrates that it is both possible and practical to find an improved treatment that provides a significant improvement over current practice despite not being the true optimal treatment. It is almost certainly possible to devise a targeting method based on structural data, which is yet more effective.

In addition to structure-guided BT, the utility of functional image-guided BT was examined whereby functional defects at specific anatomical sites were used to inform BT treatment, comparable to the information provided by functional imaging techniques such as Xe or He MRI (6, 33). In contrast to structure-guided BT, our version of functional image-guided BT (FIG) showed no improvement over conventional therapy. However, a more detailed analysis of the model output identifies potential reasons for the poor response to functional image-guided BT and from which we are able to make recommendations for refinement. The inverse correlation between (CCP1-FIG1) and control R suggests that FIG1 is more effective, relative to CCP1, in patients with better pre-treatment function. The model further reveals that FIG at times fails by selecting airways for treatment with very low ventilation before treatment which do not improve significantly post-treatment. That is, airways with the lowest ventilation are not necessarily those which show the greatest response to treatment. The functional image-guided approach may therefore require more subtlety, perhaps selecting for treatment moderately low ventilation segments which can be significantly improved, rather than the very lowest and potentially unresponsive ventilation segments. The systematic relationship between CCP1-FIG1 and control R is further relevant for the design and interpretation of future clinical trials; for example, subject exclusion criteria could bias patient response toward one end of this response spectrum.

It is also important to emphasize that we have only considered one specific algorithm for target airway selection based on functional data, and that alterations to this protocol might result in improved FIG efficacy. Indeed our efforts to categorize the relative failure of this version of FIG BT may help to define different imaging metrics to utilize the relatively ready availability of ventilation images, compared with the difficulty of obtaining extensive structural data. Finally, it is worth reiterating that our functional image-guided treatments are based directly on function, rather than from an imaging-based approximation of function. That is, we assume that Xe or He or MRI is able to accurately capture functional flow information—we use the latter directly in the model, while in clinical

practice the former would be used. There are certainly questions on the extent to which imaging accurately captures function, which would be an additional determinant of functional image-guided BT efficacy in clinical practice.

Taken together, the results of a new and sophisticated predictive model suggest that a patient-specific, personalized medicine approach to bronchial thermoplasty is possible by appropriately selecting target airways for thermal treatment. Such predictions are made possible through understanding of the underlying mechanisms, namely that structural alteration of the treated airways alone is sufficient to alter flow patterns globally, with functional effects propagating toward the periphery and reducing overall spatial flow heterogeneity. The use of such methods, coupled with structural data, demonstrated that structure-guided BT is a promising avenue for improved therapy, while functional image-guided therapy may require further refinement, either by way of patient phenotyping or perhaps a more sophisticated method of selecting airways to be treated based on functional outcomes.

APPENDIX

This APPENDIX contains additional details on structure-guided BT methodology as well as Figs. A1, A2, and A3.

The algorithm used for structure-guided treatments SG1 and SG3 is described briefly in the main text, and additional details are provided in this APPENDIX. For each simulated patient, a set of potential treatment airways is considered. The constraints on selecting the airways to be treated are as follows:

- The airways must be sufficiently large to be treatable.
- There must be enough potential airways in the treatment set such that the choice of airways finally treated is not unduly constrained.
- The number of potential treatment airways is not so large as to be computationally infeasible.

On balance, we used the 75 largest airways as our possible treatment set, but for generality we shall call the number of potential treatment airways M .

For each airway in the potential treatment set, which we refer to as “airway i ”, we use the predictive model (described in the main text) to determine the outcome of a BT procedure that treats only that airway and its proximal flow pathway. The resulting impedance of that treatment is calculated and compared with the pretreatment control to determine the associated change in resistance, referred to as “ ΔR_i ”; e.g., the change in resistance associated with treatment of the i th possible treatment. Although this must be done for each of the M potential treatment airways, importantly, all such assessments are independent and so can be calculated in parallel².

Having computed all of the ΔR_i for $i = 1, \dots, M$, we then perform a ranking of the potential treatment airways for treatment priority based on their response. For a treatment of N airways, then, we select the largest N responses and select for treatment their associated airways. As a final check, the simulated function (resistance at 6 Hz) for this N airway treatment is compared with the predictions for standard clinical practice (e.g., CCP1 or CCP3 as comparison for either SG1 or SG3, respectively). In the event that the airway treatment interactions are sufficiently nonlinear that this approach is not predicted to be superior to the standard approach (CCP1/3), the latter is used instead. For this relatively simple approach with a single potential treatment airway being associated with a single output measure, a straight ranking of responses is possible; for more complex versions potentially trialing multiple potential target airways and/or multiple output

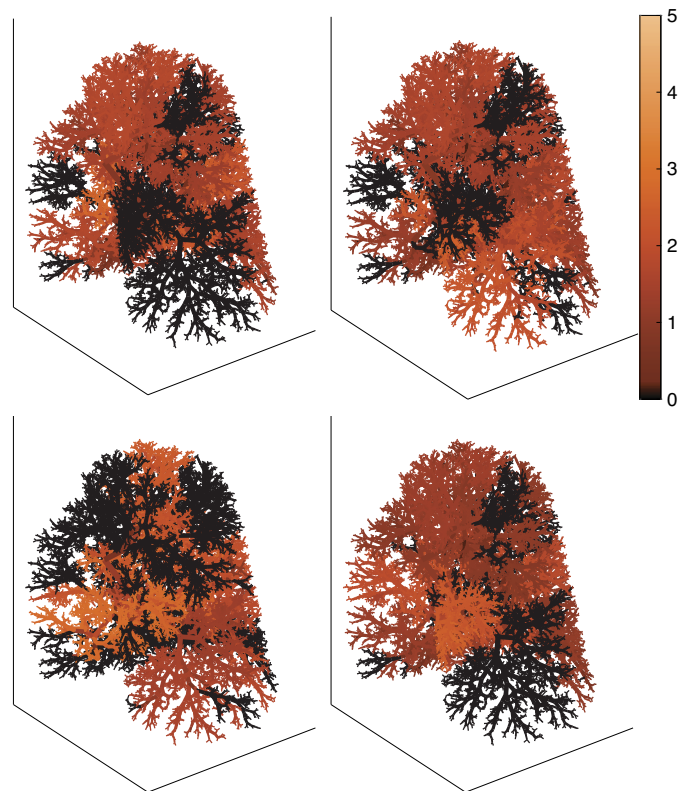


Fig. A1. Flow patterns from *simulated patient no. 1*, extended from Fig. 1. *Top left*: functional image-guided bronchial thermoplasty 1 (FIG1). *Top right*: current clinical practice (CCP3). *Bottom left*: functional image-guided bronchial thermoplasty 3 (FIG3). *Bottom right*: structure-guided bronchial thermoplasty 3 (SG3). Details otherwise as in Fig. 1.

measures, the singular value decomposition, akin to principal component analysis, might be used to estimate the optimal treatment set.

ACKNOWLEDGMENTS

We thank Artee Karkhanis, Marija Sunjar, Hannah Park, and Salima Harji for expert technical assistance with collecting, processing, and performing morphometric analyses on the autopsy lungs. We also thank the families of the deceased subjects for consenting to this study and providing demographic and medical information.

GRANTS

Supported by the Royal Society of New Zealand via the Marsden Fund (to G. M. Donovan).

DISCLOSURES

No conflicts of interest, financial or otherwise, are declared by the authors.

AUTHOR CONTRIBUTIONS

G.M.D. conceived and designed research; G.M.D., J.G.E., S.R.B., and F.H.G. performed experiments; G.M.D. analyzed data; G.M.D., A.L.J., and P.B.N. interpreted results of experiments; G.M.D. prepared figures; G.M.D., J.G.E., and P.B.N. drafted manuscript; G.M.D., J.G.E., F.H.G., A.L.J., and P.B.N. edited and revised manuscript; G.M.D., J.G.E., S.R.B., F.H.G., A.L.J., and P.B.N. approved final version of manuscript.

REFERENCES

1. Adams DC, Hariri LP, Miller AJ, Wang Y, Cho JL, Villiger M, Holz JA, Szabari MV, Hamilos DL, Scott Harris R, Griffith JW, Bouma BE, Luster AD, Medoff BD, Suter MJ. Birefringence microscopy platform for assessing airway smooth muscle structure and

² Given current computational constraints, a series calculation of this magnitude would be impractical.

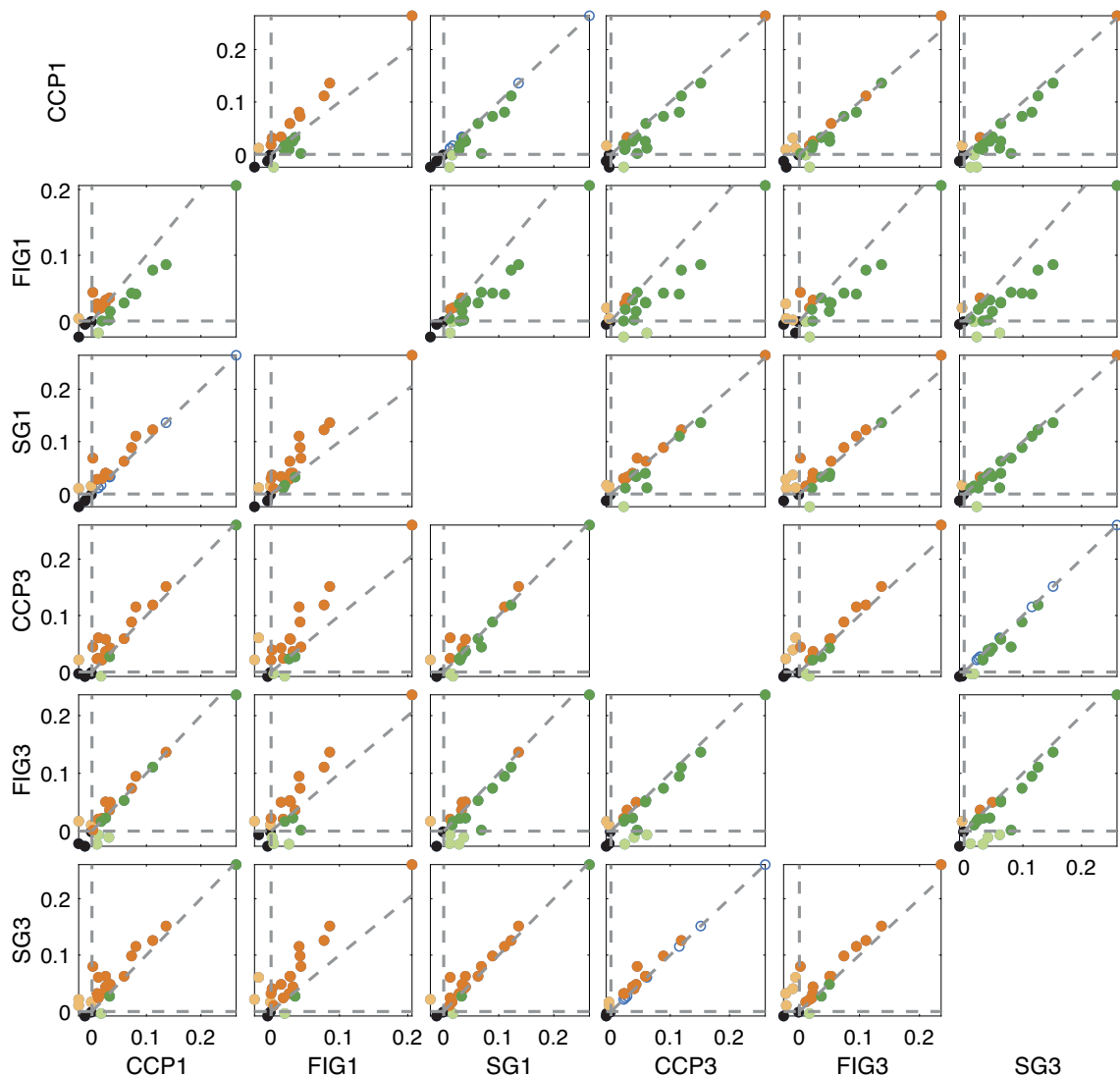


Fig. A2. Differential response of each treatment (in terms of change in R). Color coding as follows: orange: y-axis treatment is superior to x-axis treatment; green: x-axis treatment is superior to y-axis treatment; black: neither treatment improves function; blue: both treatments are equivalent.

- function in vivo. *Sci Transl Med* 8: 359ra131, 2016. doi:10.1126/scitranslmed.aag1424.
- Anafi RC, Wilson TA. Airway stability and heterogeneity in the constricted lung. *J Appl Physiol* (1985) 91: 1185–1192, 2001. doi:10.1152/jap.2001.91.3.1185.
 - Bicknell S, Chaudhuri R, Thomson NC. How to: Bronchial thermoplasty in asthma. *Breathe* (Sheff) 10: 48–59, 2014. doi:10.1183/20734735.007813.
 - Brown RH, Wizeman W, Danek C, Mitzner W. In vivo evaluation of the effectiveness of bronchial thermoplasty with computed tomography. *J Appl Physiol* (1985) 98: 1603–1606, 2005. doi:10.1152/jap.2005.01210.2004.
 - Burrows KS, De Backer J, Smallwood R, Sterk PJ, Gut I, Wirix-Speetjens R, Siddiqui S, Owers-Bradley J, Wild J, Maier D, Brightling C. Multi-scale computational models of the airways to unravel the pathophysiological mechanisms in asthma and chronic obstructive pulmonary disease (AirPROM). *Interface Focus* 3: 20120057, 2013. doi:10.1098/rsfs.2012.0057.
 - Castro M, Fain SB, Hoffman EA, Gierada DS, Erzurum SC, Wenzel S; National Heart, Lung, and Blood Institute's Severe Asthma Research Program. Lung imaging in asthmatic patients: the picture is clearer. *J Allergy Clin Immunol* 128: 467–478, 2011. doi:10.1016/j.jaci.2011.04.051.
 - Castro M, Rubin AS, Laviolette M, Fiterman J, De Andrade Lima M, Shah PL, Fiss E, Olivenstein R, Thomson NC, Niven RM, Pavord ID, Simoff M, Duhamel DR, McEvoy C, Barbers R, Ten Hacken NHT, Wechsler ME, Holmes M, Phillips MJ, Erzurum S, Lunn W, Israel E, Jarjour N, Kraft M, Shargill NS, Quiring J, Berry SM, Cox G; AIR2 Trial Study Group. Effectiveness and safety of bronchial thermoplasty in the treatment of severe asthma: a multicenter, randomized, double-blind, sham-controlled clinical trial. *Am J Respir Crit Care Med* 181: 116–124, 2010. doi:10.1164/rccm.200903-0354OC.
 - Chernyavsky IL, Russell RJ, Saunders RM, Morris GE, Berair R, Singapuri A, Chachi L, Mansur AH, Howarth PH, Dennison P, Chaudhuri R, Bicknell S, Rose FRAJ, Siddiqui S, Brook BS, Brightling CE. In vitro, in silico and in vivo study challenges the impact of bronchial thermoplasty on acute airway smooth muscle mass loss. *Eur Respir J* 51: 1701680, 2018. doi:10.1183/13993003.01680-2017.
 - Cox G, Thomson NC, Rubin AS, Niven RM, Corris PA, Sierstedt HC, Olivenstein R, Pavord ID, McCormack D, Chaudhuri R, Miller JD, Laviolette M; AIR Trial Study Group. Asthma control during the year after bronchial thermoplasty. *N Engl J Med* 356: 1327–1337, 2007. doi:10.1056/NEJMoa064707.
 - Donovan GM. Clustered ventilation defects and bilinear respiratory reactance in asthma. *J Theor Biol* 406: 166–175, 2016. doi:10.1016/j.jtbi.2016.06.035.
 - Donovan GM, Elliot JG, Green FHY, James AL, Noble PB. Unraveling a Clinical Paradox: Why Does Bronchial Thermoplasty Work in Asthma? *Am J Respir Cell Mol Biol* 59: 355–362, 2018. doi:10.1165/rcmb.2018-0011OC.

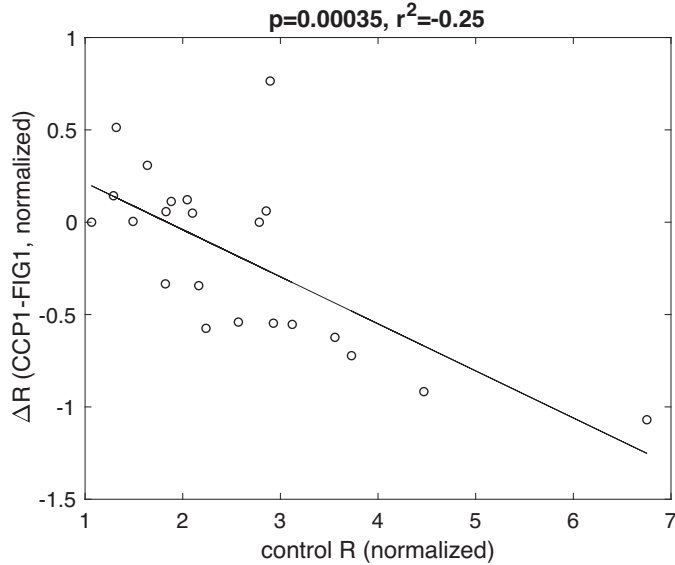


Fig. A3. Differential response between current clinical practice 1 (CCP1) and functional image-guided bronchial thermoplasty 1 (FIG1) is negatively correlated with control R.

12. Donovan GM, Kritter T. Spatial pattern formation in the lung. *J Math Biol* 70: 1119–1149, 2015. doi:10.1007/s00285-014-0792-9.
13. Dubsky S, Zosky GR, Perks K, Samarage CR, Henon Y, Hooper SB, Fouras A. Assessment of airway response distribution and paradoxical airway dilation in mice during methacholine challenge. *J Appl Physiol* (1985) 122: 503–510, 2017. doi:10.1152/jappphysiol.00476.2016.
14. Elliot JG, Jones RL, Abramson MJ, Green FH, Mauad T, McKay KO, Bai TR, James AL. Distribution of airway smooth muscle remodelling in asthma: relation to airway inflammation. *Respirology* 20: 66–72, 2015. doi:10.1111/resp.12384.
15. Elliot JG, Budgeon CA, Harji S, Jones RL, James AL, Green FH. The effect of asthma on the perimeter of the airway basement membrane. *J Appl Physiol* (1985) 119: 1114–1117, 2015. doi:10.1152/jappphysiol.00076.2015.
16. Green FHY, Williams DJ, James A, McPhee LJ, Mitchell I, Mauad T. Increased myoepithelial cells of bronchial submucosal glands in fatal asthma. *Thorax* 65: 32–38, 2010. doi:10.1136/thx.2008.111435.
17. Hall C, Nici L, Sood S, ZuWallack R, Castro M. Nonpharmacologic Therapy for Severe Persistent Asthma. *J Allergy Clin Immunol Pract* 5: 928–935, 2017. doi:10.1016/j.jaip.2017.04.030.
18. Hessel PA, Mitchell I, Tough S, Green FHY, Cockcroft D, Kepron W, Butt JC; Prairie Provinces Asthma Study Group. Risk factors for death from asthma. *Ann Allergy Asthma Immunol* 83: 362–368, 1999. doi:10.1016/S1081-1206(10)62832-3.
19. d'Hooghe JNS, Ten Hacken NHT, Weersink EJM, Sterk PJ, Annema JT, Bonta PI. Emerging understanding of the mechanism of action of Bronchial Thermoplasty in asthma. *Pharmacol Ther* 181: 101–107, 2018. doi:10.1016/j.pharmthera.2017.07.015.
20. Horsfield K. Diameters, generations, and orders of branches in the bronchial tree. *J Appl Physiol* (1985) 68: 457–461, 1990. doi:10.1152/jappphysiol.1990.68.2.457.
21. King GG, Noble PB. Airway remodelling in asthma: It's not going away. *Respirology* 21: 203–204, 2016. doi:10.1111/resp.12727.
22. Kirby M, Ohtani K, Lopez Lisbona RM, Lee AMD, Zhang W, Lane P, Varfolomeva N, Hui L, Inescu D, Coxson HO, MacAulay C, FitzGerald JM, Lam S. Bronchial thermoplasty in asthma: 2-year follow-up using optical coherence tomography. *Eur Respir J* 46: 859–862, 2015. doi:10.1183/09031936.00016815.
23. Langton D, Ing A, Fielding D, Wang W, Plummer V, Thien F. Bronchodilator responsiveness as a predictor of success for bronchial thermoplasty. *Respirology* 24: 63–67, 2019. doi:10.1111/resp.13375.
24. Leary D, Winkler T, Braune A, Maksym GN. Effects of airway tree asymmetry on the emergence and spatial persistence of ventilation defects. *J Appl Physiol* (1985) 117: 353–362, 2014. doi:10.1152/jappphysiol.00881.2013.
25. Li Q, Karnowski K, Noble PB, Cairncross A, James A, Villiger M, Sampson DD. Robust reconstruction of local optic axis orientation with fiber-based polarization-sensitive optical coherence tomography. *Biomed Opt Express* 9: 5437–5455, 2018. doi:10.1364/BOE.9.005437.
26. Lutchen KR, Gillis H. Relationship between heterogeneous changes in airway morphometry and lung resistance and elastance. *J Appl Physiol* (1985) 83: 1192–1201, 1997. doi:10.1152/jappphysiol.1997.83.4.1192.
27. Paré PD, Mitzner W. Airway-parenchymal interdependence. *Compr Physiol* 2: 1921–1935, 2012. doi:10.1002/cphy.c110039.
28. Pavord ID, Cox G, Thomson NC, Rubin AS, Corris PA, Niven RM, Chung KF, Laviolette M; RISA Trial Study Group. Safety and efficacy of bronchial thermoplasty in symptomatic, severe asthma. *Am J Respir Crit Care Med* 176: 1185–1191, 2007. doi:10.1164/rccm.200704-571OC.
29. Pretolani M, Bergqvist A, Thabut G, Dombret M-C, Knapp D, Hamidi F, Alavoine L, Taillé C, Chanez P, Erjefält JS, Aubier M. Effectiveness of bronchial thermoplasty in patients with severe refractory asthma: Clinical and histopathologic correlations. *J Allergy Clin Immunol* 139: 1176–1185, 2017. doi:10.1016/j.jaci.2016.08.009.
30. Pretolani M, Dombret MC, Thabut G, Knap D, Hamidi F, Debray M-P, Taille C, Chanez P, Aubier M. Reduction of airway smooth muscle mass by bronchial thermoplasty in patients with severe asthma. *Am J Respir Crit Care Med* 190: 1452–1454, 2014. doi:10.1164/rccm.201407-1374LE.
31. Salkie ML, Mitchell I, Revers CW, Karkhanis A, Butt J, Tough S, Green FH. Postmortem serum levels of tryptase and total and specific IgE in fatal asthma. *Allergy Asthma Proc* 19: 131–133, 1998. doi:10.2500/108854198778604121.
32. Saragaglia A, Fetita C, Brillet PY, Prêteux F, Grenier PA. Airway wall thickness assessment: a new functionality in virtual bronchoscopy investigation. *Proc SPIE* 6511: 1–12, 2007. doi:10.1117/12.709532.
33. Svenningsen S, Kirby M, Starr D, Leary D, Wheatley A, Maksym GN, McCormack DG, Parraga G. Hyperpolarized (3) He and (129) Xe MRI: differences in asthma before bronchodilation. *J Magn Reson Imaging* 38: 1521–1530, 2013. doi:10.1002/jmri.24111.
34. Thomen RP, Sheshadri A, Quirk JD, Kozlowski J, Ellison HD, Szczesniak RD, Castro M, Woods JC. Regional ventilation changes in severe asthma after bronchial thermoplasty with (3)He MR imaging and CT. *Radiology* 274: 250–259, 2015. doi:10.1148/radiol.14140080.
35. Thomson NC, Rubin AS, Niven RM, Corris PA, Siersted HC, Olivenstein R, Pavord ID, McCormack D, Laviolette M, Shargill NS, Cox G; AIR Trial Study Group. Long-term (5 year) safety of bronchial thermoplasty: Asthma Intervention Research (AIR) trial. *BMC Pulm Med* 11: 8, 2011. doi:10.1186/1471-2466-11-8.
36. Thorpe CW, Bates JH. Effect of stochastic heterogeneity on lung impedance during acute bronchoconstriction: a model analysis. *J Appl Physiol* (1985) 82: 1616–1625, 1997. doi:10.1152/jappphysiol.1997.82.5.1616.
37. Tough SC, Green FHY, Paul JE, Wigle DT, Butt JC. Sudden death from asthma in 108 children and young adults. *J Asthma* 33: 179–188, 1996. doi:10.3109/02770909609054550.
38. Trivedi A, Pavord ID, Castro M. Bronchial thermoplasty and biological therapy as targeted treatments for severe uncontrolled asthma. *Lancet Respir Med* 4: 585–592, 2016. doi:10.1016/S2213-2600(16)30018-2.
39. Venegas JG, Winkler T, Musch G, Vidal Melo MF, Layfield D, Tgavalekos N, Fischman AJ, Callahan RJ, Bellani G, Harris RS. Self-organized patchiness in asthma as a prelude to catastrophic shifts. *Nature* 434: 777–782, 2005. doi:10.1038/nature03490.
40. Wechsler ME, Laviolette M, Rubin AS, Fiterman J, Lapa e Silva JR, Shah PL, Fiss E, Olivenstein R, Thomson NC, Niven RM, Pavord ID, Simoff M, Hales JB, McEvoy C, Slebos DJ, Holmes M, Phillips MJ, Erzurum SC, Hanania NA, Sumino K, Kraft M, Cox G, Sterman DH, Hogarth K, Kline JN, Mansur AH, Louie BE, Leeds WM, Barbers RG, Austin JHM, Shargill NS, Quiring J, Armstrong B, Castro M; Asthma Intervention Research 2 Trial Study Group. Bronchial thermoplasty: Long-term safety and effectiveness in patients with severe persistent asthma. *J Allergy Clin Immunol* 132: 1295–1302.e3, 2013. doi:10.1016/j.jaci.2013.08.009.
41. Wenzel SE. Asthma phenotypes: the evolution from clinical to molecular approaches. *Nat Med* 18: 716–725, 2012. doi:10.1038/nm.2678.
42. Winkler T, Venegas JG. Complex airway behavior and paradoxical responses to bronchoprovocation. *J Appl Physiol* (1985) 103: 655–663, 2007. doi:10.1152/jappphysiol.00041.2007.